Motion Parameter Estimation via Dopplerlet-Transform-Based Matched Field Processing

Hongyan Dai

Abstract— This work presents a matched field processing (MFP) algorithm based on Dopplerlet transform for estimating the motion parameters of a sound source moving along a straight line and with a constant speed by using a piecewise strategy, which can significantly reduce the computational burden. Monte Carlo simulation results and an experimental result are presented to verify the effectiveness of the algorithm advocated.

Key words—matched field processing; Dopplerlet transform; motion parameter estimation; piecewise strategy

I. INTRODUCTION

IN recent years MFP techniques proposed by Bucker [1] have been successfully applied to target motion analysis (TMA). MFP matches a measured acoustic field with a predicted field, based on a motion model of the sound source, for all possible motion parameters of an acoustic source in a search region[2]. The Dopplerlet transform [3] estimated the parameters via Matching Pursuits which adaptively decomposes any signal under analysis into a linear combination of a set of atoms that are selected from a large redundant dictionary of atoms in accordance with the criterion of maximum projection energy. Although the computations of Dopplerlet transform are carried out only on the lattice points through the discretization of parameters, the exhaustive search of a multidimensional parameter space results in heavy computational burden. In fact, all MFP techniques inherently have large computational demands, so there is an increasing interest in their efficient implementations [4]-[5]. In this paper we present an efficient MFP algorithm based on Dopplerlet transform, for estimating the motion parameters of a sound source using a single sensor, and show how the computational burden can be significantly reduced (5 to 15 times).

II. CONVENTIONAL ESTIMATION METHOD BASED ON DOPPLERLET TRANSFORM[3]

A. Dopplerlet Transform

Doppler signals are a class of signals existing in nature. Dopplerlet transform is parsimonious for delineating the time-varying spectral contents of such Doppler-like signals. The Dopplerlet transform of any square-integrable signal $s(t) \in$

H. Dai is with the Department of Automation, Tsinghua University, Beijing 100084, China (e-mail: daihy04@mails.tsinghua.edu.cn).

$L^2(\mathbb{R})$ may be readily defined as

$$
\begin{aligned}
&\mathrm{DT}_s(t_c, f_c, \log\sigma, r, v, u) \\
&= \langle s(t),\ d_{t_c, f_c, \log\sigma, r, v, u}(t) \rangle \\
&= \frac{1}{\sqrt{\sigma}} \int_{-\infty}^{\infty} s(\nu) \cdot g^*\left(\frac{\nu - t_c}{\sigma}\right)
\end{aligned}
\tag{1}
$$

$$
\cdot\exp\left\{-j2\pi u\left[u + \frac{v^2\left(\frac{\nu - t_c}{\sigma}\right)}{\sqrt{r^2 + v^2\left(\frac{\nu - t_c}{\sigma}\right)^2}}\right]^{-1} f_c \cdot \left(\frac{\nu - t_c}{\sigma}\right)\right\} d\nu
\tag{2}
$$

where $j = \sqrt{-1}$, $\sigma \in \mathbb{R}^+$, $u \in \mathbb{R}^+$, $(t_c, f_c) \in \mathbb{R}^2$, $l \geqslant 0$, $u > v \geqslant 0$, "$\langle,\rangle$" denotes the Dirac inner product and the superscript "$*$" denotes the complex conjugate operation. Clearly, such a Dopplerlet is dictated by, besides the shape of $g(t)$, the following six parameters that each has an intuitively satisfying significance: time center t_c, frequency center f_c, log duration $\log\sigma$ (note that if $\sum \log\sigma$ is an arithmetic progression, then $\sum \sigma$ is a geometric progression, thereby σ denotes the dilation), distance r between the observer and the line that the source moves along, source speed v, and wave propagation speed u. The motion parameter set is denoted as $\gamma = (t_c, f_c, r, v, u)$.

B. Energy-Based MFP Algorithm

The (complex) Dopplerlet transform can be written concisely in the form

$$
\mathrm{DT}_s(\gamma) = \langle s(t),\ d(t) \rangle.
\tag{3}
$$

Then, signal s can be decomposed into

$$
s = \langle s,\ d \rangle d + R_s
\tag{4}
$$

where $\langle s,\ d \rangle d$ is the projection of s in the direction of d, R_s is its corresponding residual signal. The matching-pursuit-based Dopplerlet transform is an iterative projection algorithm that subdecomposes the residual signal R_s by projecting it on a vector that matches R_s almost at best, as was done for s in (4). After each iteration, a Dopplerlet atom that best matched the dominating component of residual signal is selected. The decomposition process is iterated until the residual energy is below some threshold or until some other halting criterion is met.

When we apply the above-mentioned algorithm to the scenario of estimating a sound source moving along a straight line and with a constant speed, we will get only one selected Dopplerlet atom. Then, the motion parameters according to this Dopplerlet atom is what we want.

III. Efficient Implementation

A. Replica Model

According to Eq. (2), for an assumed motion parameter space $\mathbf{\Gamma}$, the replicas are formed by the product of the magnitude envelop $a_m(t_i)$ and the frequency $f_m(t_i)$ plus white noise $n(t_i) \sim \mathcal{N}(0, \sigma_n^2)$

$$s(t_i) = d(t_i) + n(t_i) \tag{5}$$
$$= a_m(t_i) \cdot f_m(t_i) + n(t_i) \tag{6}$$

where

$$a_m(t_i) = \frac{1}{\sqrt{D}} \tag{7}$$

$$f_m(t_i) = \cos\left\{ j2\pi f_c \left[1 + \frac{v^2(t_i - t_c)}{u \cdot D} \right]^{-1} (t_i - t_c) \right\} \tag{8}$$

$$D = \sqrt{r^2 + [v(t_i - t_c)]^2}, \quad i = 1, 2, \cdots, NK. \tag{9}$$

Fig. 1 shows a Doppler signal according to Eq. (6) ($\sigma_n^2 = 0$).
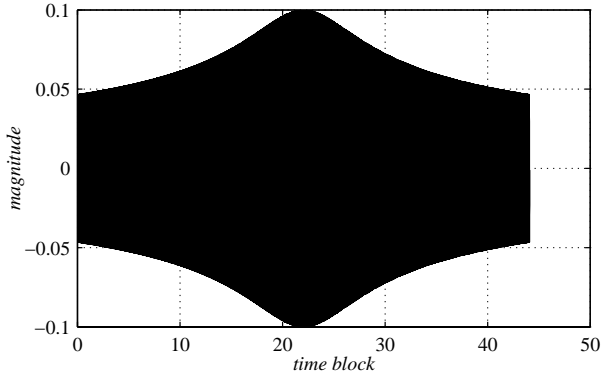

Fig. 1.   Doppler signal without noise.

B. Frequency Energy Distribution Curve

We can divide a Doppler signal $s(t)$ according to Eq. (6) into K time blocks, and each time block has N data points and a time duration $T = N/\text{Fs}$ s, where Fs is the sampling frequency.

Note that each time block is assumed to be quasi-stationarity, *viz*, the magnitude change is small and the frequency may approximate to constant, which guarantees the main frequency energy in each time block concentrates in a narrow frequency band. So T should be chosen small enough to meet the quasi-stationarity approximation but large enough in order that the overall number of time blocks is small enough that the matching process is computationally feasible.

Let R_f be the frequency resolution and $\triangle f$ be the overall frequency change owing to Doppler effect, then we may choose Fs and N to uphold the following condition

$$R_f = \frac{\text{Fs}}{N} = \triangle f \tag{10}$$

which may ensure that the main frequency energy of each time block concentrates in a narrow frequency band centered in f_c.

Carrying out the Discrete Fourier Transform (DFT) on each time block of the replica, and the largest complex number in each DFT sequence f is defined as DFT factor. Then, we will get a sequence $F = [f(1), f(2), \cdots, f(K)]$, called frequency energy distribution curve, representing change of the main frequency energy in each time block. We may get L curves $F_l = [f_l(1), f_l(2), \cdots, f_l(K)]$ in the search space $\mathbf{\Gamma}$, where $l = 1, 2, \cdots, L$.

Following the above-mentioned process, we may also get the frequency energy distribution curve of the received signal $s'(t)$, $F' = [f'(1), f'(2), \cdots, f'(K)]$.

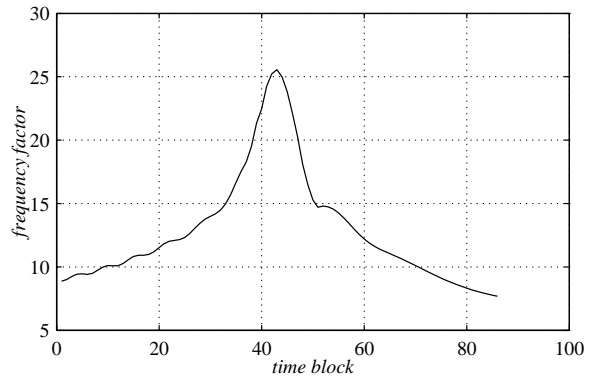Fig. 2 shows the frequency energy distribution curve of the signal in Fig. 1.

Fig. 2.   Frequency energy distribution curve of the signal in Fig. 1.

C. Effects of DFT

The DFT has two effects here. First, an entire time block of N samples is reduced to a single complex number $f(k)$, and its absolute value represents the frequency energy in a narrowband in kth time block, the validation of which is guaranteed by Eq. (10). This enables matching process to be performed in a far smaller data set, therefor vastly decreasing the computational burden. Second, as the white noise energy distributes uniformly in the frequency domain and the main frequency energy of the signal is in a narrowband, the white noise energy in this narrowband is quite small. In this sense, DFT suppress white noise.

Fig. 3 is the signal in Fig. 1 with the signal-to-noise ratio (SNR) 1 dB and its frequency energy distribution curve is shown in Fig. 4.

As we can see in Fig. 3, due to white noise effect, the signal is so ambiguous that it loses its Doppler characteristic, which limits the adaption of energy matching in time domain. However, the frequency energy distribution curve is just less sleek and keeps the essence variation of the main frequency energy.
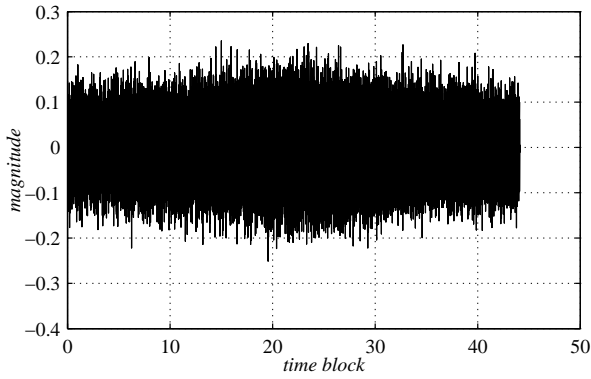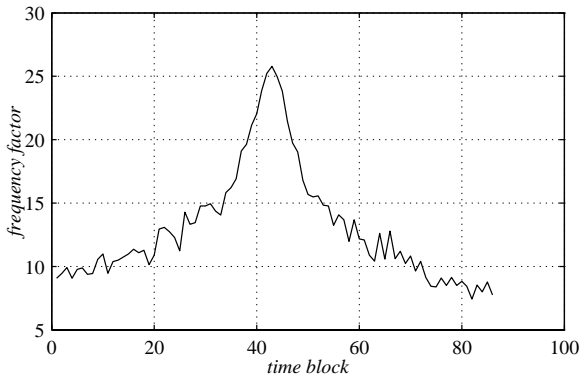
Fig. 3. Doppler signal with SNR = 1 dB.

Fig. 4. Frequency energy distribution curve of the signal in Fig. 3.

IV. MFP ALGORITHM

A. Cost Function

The correlation coefficients of the frequency energy distribution curves between the received signal and the replicas show the similarity degree of actual motion parameters and the estimation ones. t_c, f_c, r, v and u corresponding to the replica with the largest correlation coefficient of frequency energy distribution curve between the received signal and the replica, are the very parameters we want. The cost function for matching data between received signal and an assumed set of replicas is

$$C_l'(k) = \frac{|F'(k)| \cdot |F_l(k)|^\text{T}}{\| |F'(k)| \|_2 \cdot \| |F_l(k)| \|_2} \qquad (11)$$

where $F'(k) = [f'(1), f'(2), \cdots, f'(k)]$, $F_l(k) = [f_l(1), f_l(2), \cdots, f_l(k)]$, "$| \cdot |$" denotes the absolute value, "$\| \cdot \|$" denotes the usual L^2-norm and superscript "T" denotes the transpose operation.

As $C_l'(k) \leq 1$, we change Eq. (11) to

$$C_l(k) = C_l'(k) \cdot C_l'(k-1) \cdot \cdots \cdot C_l'(1). \qquad (12)$$

Then, the cost scores in Eq. (12) according to the curve with incorrect parameters will reduce more quickly over time. This cost function is maximised over the parameter space $\mathbf{\Gamma}$.

In a parameter space composed of all possible combinations of motion parameters, incorrect replicas will often yield poor scores after a small number of time blocks. Fig. 5 shows the match scores for 441 replicas with a noise-free simulated Doppler signal. As we can see in this figure, many of the replicas yield poor scores after the first 50 time blocks. None of these are likely to be the successful replicas and thus the computations are wasted if these replicas are matched in the entire parameter space $\mathbf{\Gamma}$. We could compute the cost function Eq. (12) at each consecutive time block, discarding the candidates with poor cost scores, which has the potential to decrease the computations required to find the best replica.
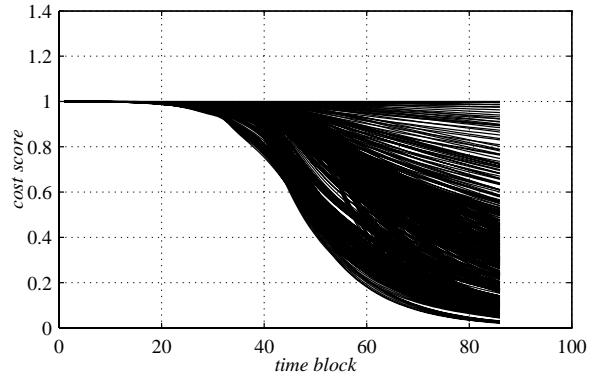

Fig. 5. Match scores for 441 replicas with a noise-free simulated Doppler signal.

This batch process would involve recomputing the correlation coefficient at each time, which is also wasteful. Iterative strategy by updating the scores from previous time block, can surmount this drawback, thereby leading to an efficient algorithm for matching process.

We can rewrite Eq. (11) as:

$$C_l'(k) = \frac{\alpha_l(k)}{\sqrt{\beta_l(k)} \cdot \sqrt{\eta_l(k)}} \qquad (13)$$

where

$$\alpha_l(k) = |f'(1)||f_l(1)| + |f'(2)||f_l(2)| + \cdots + |f'(k)||f_l(k)| \qquad (14)$$

$$\beta_l(k) = |f'(1)|^2 + |f'(2)|^2 + \cdots + |f'(k)|^2 \qquad (15)$$

$$\eta_l(k) = |f_l(1)|^2 + |f_l(2)|^2 + \cdots + |f_l(k)|^2. \qquad (16)$$

It is clear that $\alpha_l(k)$, $\beta_l(k)$ and $\eta_l(k)$ can be expressed in terms of $\alpha_l(k-1)$, $\beta_l(k-1)$ and $\eta_l(k-1)$ as follows

$$\alpha_l(k) = \alpha_l(k-1) + |f'(k)||f_l(k)| \qquad (17)$$

$$\beta_l(k) = \beta_l(k-1) + |f'(k)|^2 \qquad (18)$$

$$\eta_l(k) = \eta_l(k-1) + |f_l(k)|^2. \qquad (19)$$

The cost function Eq. (13) for kth time block can now be expressed as

$$C_l'(k) = \frac{\alpha_l(k-1) + |f'(k)||f_l(k)|}{\sqrt{\beta_l(k-1) + |f'(k)|^2} \cdot \sqrt{\eta_l(k-1) + |f_l(k)|^2}}. \qquad (20)$$

By substituting Eq. (20) into Eq. (12), we can compute the cost scores in an iterative and parallel manner as more data becomes available, which first results in decrease in storage requirements.

B. Discard Threshold

As the maximum of the cost score is 1, when the cost score in kth time block decrease $1/K$ than that in $(k$-1)th time block, or the cost score is under the threshold T_h, the replica d_l should be discarded. The discard criteria is as follows:

$$\frac{C_l(k) - C_l(k-1)}{C_l(k)} > \frac{1}{K} \qquad (21)$$
$$\text{or} \qquad C_l(k) \leq T_h.$$

C. Fast MFP Algorithm

We can use coarse to fine matching strategy to ulteriorly decrease the computational burden. An algorithm to implement the matching process in an efficient manner can thus be specified as follows.

1) Coarse matching.

Guess the initial values of the parameters, determine reasonably the rough parameter intervals for matching, and use relatively big and fixed matching steps, thus, forming the candidate coarse search space Γ_1.

a) Iterate over each of the K time blocks. In the kth time block,

   i) Compute the DFT factor of the received signal $f'(k)$;

   ii) Form the replica $[d(t_{(k-1)N+1}) \cdots d(t_{kN})]$ according to Eq. (6);

   iii) Compute the DFT factor of each replica $f_l(k)$;

   iv) Update $\alpha_l(k)$, $\beta_l(k)$ and $\eta_l(k)$ according to Eq. (17), (18) and (19), respectively;

   v) Compute the cost score for each replica $C_l(k)$ according to Eq. (12);

   vi) Discard the replicas that do not satisfy the discard criteria, and replace the current parameter set γ_1

$$\Gamma_1 = \{\gamma_1 \in \Gamma_1 \mid$$
$$\frac{C_l(k)-C_l(k-1)}{C_l(k)} > \frac{1}{K} \quad \text{or} \quad C_l(k) \leq T_h\};$$

b) Process the next time block $k = k + 1$.

2) Fine matching.

After finishing coarse matching, we get the coarsely estimated parameter set $\tilde{\gamma} = (\tilde{t}_c, \tilde{f}_c, \tilde{r}, \tilde{v}, \tilde{u})$. To find a Dopplerlet atom that matches the signal even better, we then perform the numerical optimization by searching for the parameters in a neighborhood of $\tilde{\gamma}$ in much smaller searching steps to reach a local maxima. The candidate coarse search space is Γ_2. The detail matching process is the same as that of coarse matching. Denote the fine parameter set as $\hat{\gamma} = (\hat{t}_c, \hat{f}_c, \hat{r}, \hat{v}, \hat{u})$.

D. Speed Gain

We expect an improvement in the matching speed inherent in the FFT-based processing schemes. The ratio of the computation load in conventional method, i.e., computing the replica field for each trial motion parameter and then computing the Dirac inner product in time domain[3], to that in this FMFP is given by

$$\text{Speed Gain} \approx \frac{(L_1 + L_2) \cdot K \cdot N}{(1 + K) \sum_{k=1}^{K} \{k [L_{d1}(k) + L_{d2}(k)]\}} \quad (22)$$

where L_1 and L_2 are the number of replicas of coarse and fine matching, respectively, and $L_{d1}(k)$ and $L_{d2}(k)$ are the number of discarded replica in kth time block of coarse and fine matching, respectively. Note that we suppose the computations of N points DFT approximate to those of K points inner product.

V. APPLICATION

In this section we present simulation results using computer-generated signals and an experimental result to verify the effectiveness of this matched field processing algorithm using a single sensor.

A. Simulation

To demonstrate the feasibility of this matching algorithm, we performed a simulation test using a computer-generated signal. Suppose that the underwater source moves along a straight line with speed $v = 45$ m/s, distance $r = 100$ m, center frequency $f_c = 60$ Hz, wave propagation $u = 1440$ m/s (usually, the wave speed is known), time center $t_c = 5$ s (which amounts to a signal duration of $t = 10$ s) and time duration of each time block $T = 0.05$ s.

The coarse matching process without discard is shown in Fig. 5. Following the above discard criteria, assume the threshold $T_h = 0.5$, the coarse matching process is shown in Fig. 6 and the histogram of discard occurrence is in shown Fig. 7, where the matching steps for t_c, f_c, r, v, respectively, are 1 s, 5 Hz, 5 m and 5 m/s. As we can see in Fig. 7, after
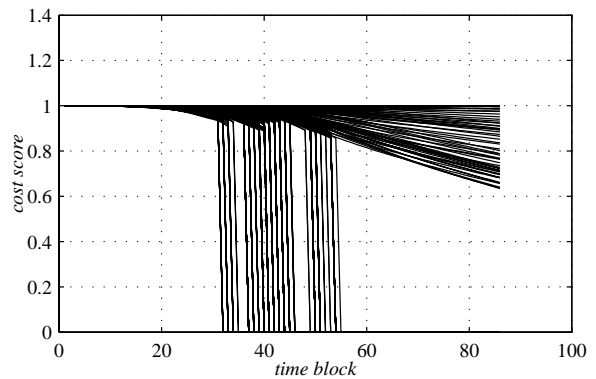

Fig. 6.   Coarse matching process with discard.

50th time block, there leaves only 20% replicas. The coarse match result $\tilde{\gamma} = (\tilde{t}_c, \tilde{f}_c, \tilde{r}, \tilde{v}, \tilde{u}) = (10.8, 64, 96, 43, 1440)$.
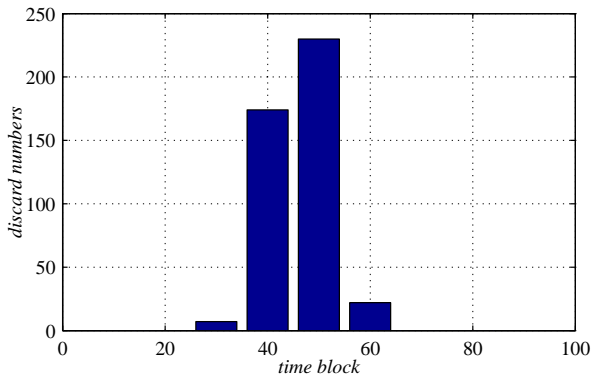
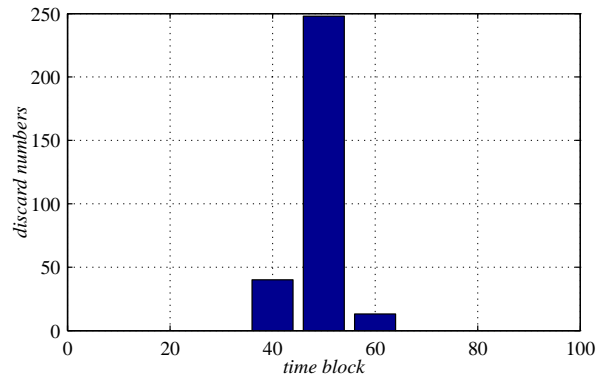Fig. 7.   Histogram of discard occurrence (coarse matching).

Fig. 9.   Histogram of discard occurrence (fine matching).

The fine matching process is shown in Fig. 8 and the histogram of discard occurrence is shown in Fig. 9, where the matching steps for t_c, f_c, r, v, respectively, are 0.2 s, 1 Hz, 1 m and 1 m/s. The match result is $\hat{\gamma} = (\hat{t_c}, \hat{f_c}, \hat{r}, \hat{v}, \hat{u}) = (10, 60, 100, 45, 1440)$.
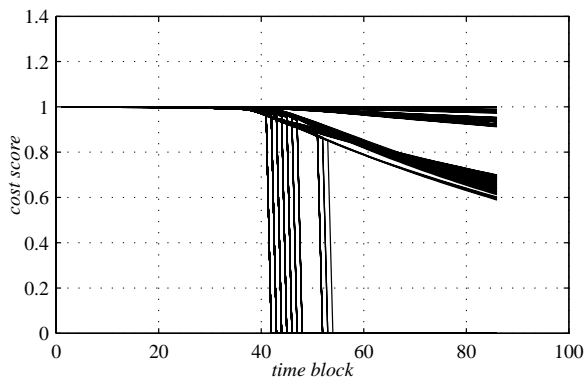

Fig. 8.   Refinement matching process with discard.

TABLE I

MEANS AND STANDARD DEVIATIONS (STDS) OF THE ESTIMATED $\hat{t}_c$, $\hat{f}_c$, $\hat{r}$ AND $\hat{v}$ UNDER DIFFERENT SIGNAL-TO-NOISE RATIOS (SNRS)

SNR (dB)	-5.00	0.00	5.00	10.00
Mean of t_c (m)	10.73	10.46	10.07	10.00
STD of t_c (m)	0.79	0.56	0.48	0.00
Mean of f_c (m/s)	55.56	61.28	60.10	59.80
STD of f_c (m/s)	5.76	3.37	2.40	0.41
Mean of r (m)	101.14	101.06	100.84	100.45
STD of r (m)	3.27	2.12	1.73	1.27
Mean of v (m)	49.92	46.44	43.74	44.40
STD of v (m)	3.60	3.10	2.76	1.23
Speed Gain	7.91	7.83	8.38	8.53

Following Eq. (21), the speed gain of this numerical simulation is 9, which significantly reduces the computational burden.

In order to examine the performance of this method under different contaminating noises, we made trials out of 50 Monte Carlo runs using zero-mean additive uniform white noise under various SNR scenarios. The trial results are tabulated in Table I.

As can be seen from Table I that the proposed matching algorithm is quite robust to noise—the random noise can hardly affect the performance.

B. Processing With Real Acoustic Data

We carried out the experiment in an October day, 2004. To help illustrate the experiment system, a schematic diagram is shown in Fig. 10. In this experiment, we use two subsystems to measure the necessary parameters: recording subsystem and atmospheric data subsystem. The recording subsystem consists of a laptop computer (with a sampling frequency 22 050 Hz) and a microphone. The atmospheric data subsystem consists of a digital barometer, and a relative humidity and temperature probe (solar radiation shielded).

The jet plane moved along a straight line at a constant height $h = 100$ m, with a constant speed $v = 139$ m/s (which were obtained from instrument mounted on the jet plane). During the time of recording, the temperature was 15.5℃, barometric pressure was 76 680 Pa, relative humidity was 28.0%, and the theoretical sound speed for the given atmospheric data was 341.61 m/s. (For an easy reference of how to calculate the sound speed, see Appendix C.A of [3].)

For an explicit comparison, we tabulate in Table II the experimental results using different estimation methods. Note that the estimation precision of the results directly read from the onboard instruments is 5%, and for Dopplerlet transform [3], the estimation precision of r is 2% and that of v is 0.5%. Accordingly, we concede that the values estimated via Dopplerlet transform to be more veracious than the values
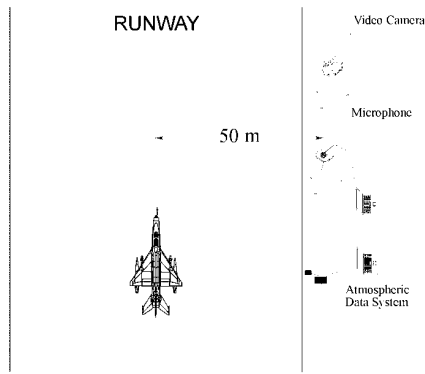
Fig. 10. Arrangement for measuring the motion parameters of a single-engine jet plane flying along a straight line at a constant height and with a constant speed.

obtained from the onboard instruments.

TABLE II
ESTIMATED RESULTS OF A FLYING JET PLANE.

Parameters	t_c (s)	f_c (Hz)	r (m)	v (m/s)	Speed Gain
Measured	\	\	112	139	\
Estimated 1	5.76	164	105	129	\
Estimated 2	5.85	167	110	128	6.45

Note: Measured: results directly read from the onboard instruments;
Estimated 1: estimated results based on Dopplerlet transform [3];
Estimated 2: estimated results based on this proposed MFP algorithm.

As can be seen from Table II, the estimation results of the proposed matching algorithm is accurate and the speed gain is 6.45, which confirms the effectiveness of the proposed matching method.

VI. CONCLUSIONS

An efficient MFP algorithm has been developed to accelerate the matching process when estimating the motion parameters based on Dopplerlet Transform. With the piecewise strategy of the cost function, the replicas with poor scores can be identified at an early iteration and excluded from further computation. We have shown that the processing speed can be considerably improved and give quantitative analysis of the computational burden reduce to make the algorithm convinced.

REFERENCES

[1] H. P. Bucker, "Use of calculated sound fields and matched field detection to locate sound sources in shallow water," *J. Acoust. Soc. Am.*, vol. 59, pp. 368-373, 1976.
[2] Michael J. Wilmut, John M. Ozard, Kyle OKeefe, and Martin Musil, " A Piecewise Matched-Field Tracking Algorithm," *IEEE J. Oceanic Engineering,* vol. 23, no. 3, pp. 167–173, 1998.
[3] H. Zou, Y. Chen, J. Zhu, Q. Dai, G. Wu, and Y. Li, "Steady-motion-based Dopplerlet transform: Application to the estimation of range and speed of a moving sound source," *IEEE J. Oceanic Engineering*, vol. 29, no. 3, pp. 887–905, 2004.
[4] S. Aravindan, N. Ramachandran, and Prabhakar S. Naidu, "Fast Matched Field Processing," *IEEE J. Oceanic Engineering*, vol. 18, no. 1, pp. 1–5, 1993.
[5] Zoi-Heleni Michalopoulou, Xiaoqun Ma, Michele Picarelli, and Urmi Ghosh-Dastidar, " Fast Matching Methods for Inversion with Underwater Sound," *IEEE J. Oceanic Engineering,* vol. 1, pp. 647–651, 2000.